Investigating the role of geo-fluvial parameters on model river banks: a flume study

Supia Khatun[1], *Mohsin* Jamal[1*], *and Md Raghib* Adil[1]

[1]Department of Civil Engineering Department, Aliah University, Kolkata, West Bengal, India

[*]**Corresponding author:** jamalmohsin15@gmail.com

Abstract: This experimental investigation aimed to analyze the failure profile of a model river bank composed of sand and silty clay. A model river bank with a length of 446 cm, a depth of 32 cm, and a slope of 1V:1.5H was prepared in a flume that was 550 cm long, 150 cm wide, and 60cm deep. Froude-number-based reduced-scale distorted river modeling was considered in this study. For modeling different parameters of flume, the linear scale 1:250 and depth scale 1:20 have been taken. The study was divided into two distinct series: Series-A and Series-B, each designed to explore specific soil types and moisture content variations. In Series-A, physical model tests were conducted using cohesionless soil (sand) with an initial moisture content set at 6% and 13%. Conversely, Series-B involved model banks constructed with silty clay soil, with initial moisture contents of 10% and 15%. Both series utilized a consistent model bank slope of 1V:1.5H. The drawdown conditions, set at 50% and 80% of the model riverbank's height, were integral to the experiments in both Series-A and Series-B. The impact of moisture content, drawdown, and bank material was observed in the failure of the model bank.

Keywords: River bank, Drawdown, Moisture content

1 Introduction

River bank erosion and collapses are a global issue, and bank collapses in India raise serious concerns for river engineering techniques. The phenomenon of bank erosion is an inherent occurrence that actively contributes to the morpho dynamics of rivers and the interconnected ecosystems surrounding them **[1].** The aforementioned process is a geomorphic phenomenon that effectively provides sediments to the river system **[2,3].** Moreover, it also facilitates the progressive sequence of riparian vegetation **[4]** and generates a diverse array of habitats for both aquatic and riparian flora and fauna **[5].**

In certain Indian states, riverbank erosion escalates into a serious environmental calamity that leads to forced migration due to the resulting socioeconomic problems and poverty **[6,7].** Land loss along river banks, particularly during the rainy season, is a nightmare for those who live beside the banks and landowners, particularly in West Bengal **[8].** Because of the loss of agricultural land, the threat to riparian areas, and the constructions on flood plains brought about by the retreat of river banks, river engineers and farmers face a critical and occasionally difficult dilemma. Thus, there is a growing body of scientific research on the failure and stability analysis of river banks and other water front slopes. Determining suitable methods for measuring bank erosion and identifying mitigation strategies require an understanding of the causes causing bank erosion **[9,10].**

The bulk of India's catastrophic mass failures of riverbanks, which are made of semi-cohesive material and alluvial or loamy sand, happen mostly when the river's water level recedes following a flood **[11].** Yazoo River Basin in Mississippi, which is one example of a system that is a victim of excessive erosion and bank instability **[12].** Properties of bank materials are important in controlling the stability of stream banks, and past studies have found that these properties are often variable spatially **[13,14,15].**

The literature underscores the necessity for a comprehensive laboratory failure study before embarking on any river bank protection project. This study is designed to elucidate the failure patterns of a model bank constructed from two distinct types of soil. Moreover, it aims to assess the suitability of the soil for simulating bank failure in a laboratory setting, mirroring real-world failure patterns. The investigation delves into the influence of moisture content, drawdown, and soil type on the alterations in profile and the location of failure.

2 Methodology

The experimental model study has been carried out to investigate the failure profile and maximum failure zone of model riverbank. The model bank was prepared in fabricated flume available in Hydraulic laboratory, Aliah University, Kolkata. For physical modelling of river bank Froude (F) similitude was used. A distorted scale of (length) 1:250 and (height) 1:20 was used for preparation of model bank. The experimental programme divided into two series, namely series-A and series-B. For series-A model banks prepared with cohesionless soil (sand) and initial moisture contents 6% and 13%. For series-B, model banks prepared with silt dominated clay soil and initial moisture contents 10% and 15%. Both series bank slope kept 1V:1.5H and drawdown ratios 50% H and 80% H.

2.1 Flume setup

The flume dimensions measure approximately 550 cm in length, 150 cm in width, and 60 cm in depth. This experimental flume incorporates an adjoining seepage area along the sides of the bank in the longitudinal direction. Within the setup, two sets of pumps have been installed to facilitate the experimentation process. A 5L/s capacity pump is dedicated to maintaining the water level in the seepage tank, simulating the water table inside the bank. Simultaneously, a 32L/s capacity pump is employed to generate channel flow. The pump capacities were meticulously determined through trial tests, ensuring the achievement of drawdown ratios from the high flood level, essential for observing failure conditions. Notably, the configuration of the setup is designed to mimic real-world scenarios closely. A visual representation of the experimental setup is provided in the accompanying figure 1.

(a)

(b)

Fig.1 Photographic view of experimental flume (a) front view (b) side view

2.2 Model Bank geometry

The experiments were conducted to examine how the failure mechanism and profile of a river bank are affected by varying drawdown ratios and different bank materials. In the laboratory, a physical model was crafted in a flume for both series, featuring a consistent 1V:1.5H slope and an identical bank height. The dimensions of the model bank geometry are detailed in the table 1, and visual representations of the bank geometries and slopes can be found in the accompanying figures 2.

Table 1 Dimensions of bank geometry for laboratory model study.

Slope of bank	Angle of slope	Height of bank (cm)	Base width of the bank (cm)
1V:1.5H	33.69^0	32	58

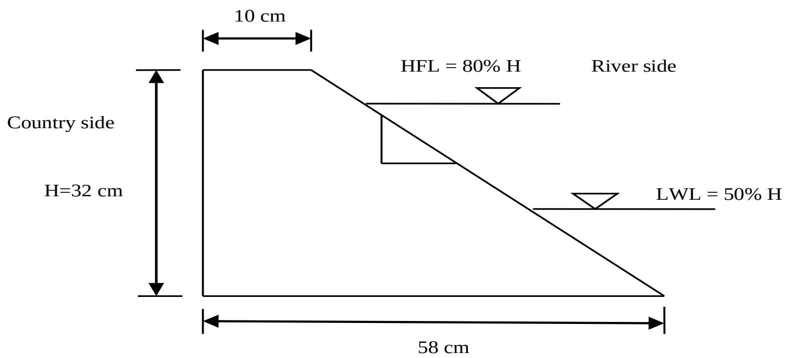

Fig.2 Geometry of model bank used in the experiment (All dimensions are in cm).

2.3 Scale parameters

The Froude-number based reduced- distorted scale has been adopted for model bank preparation in flume. A linear scale 1:250 and depth scale 1:20 was considered. The depth of water is predominant dimension in this study. The details of geometry of model and prototype was given in Table 2.

Table 2: Scale parameters

Prototype	Model
Length = 1.1 km	Length = 446 cm
Velocity = 30 cm/sec	Velocity = 6 cm/sec
Depth of river = 640 cm	Depth of river = 32 cm

2.4 Material

Two type of soil was used in this experimental study. In Series-A, cohesionless soil (sand) were used for preparation of model bank. Series-B involved model banks constructed with silty clay soil.

2.4.1. Cohesionless Soil (Sand)

In this study (Series-A), sand collected from the local site has been used as bank material. The basic geotechnical properties of the bank material have been presented in Table 3 as per IS.

Table 3 Geotechnical properties of cohesionless(sand) bank material used in the experiment.

Sl. No.	Parameters of Sand	Value and range
1	Relative Density	2.512
2	Porosity (%)	0.291
3	Angle of internal friction (ϕ) at MC=6%	32.20º
4	Angle of internal friction (ϕ) at MC=13%	34.30º
5	Bulk unit weight (γ_t) (kN/m^3) at MC=6%	15.33
6	Bulk unit weight (γ_t) (kN/m^3) at MC=13%	16.12

2.4.2. silty clay:

In Series-B, model bank prepared with silty clay type of soil. Which was collected from the -river Ganga, Kaliachak-III, Malda, West Bengal, India. As per procedure mentioned in Indian Standard code index and engineering properties of the soil has been determined. The detail of the properties is tableted below (Table 4).

Table 4 Geotechnical properties of silty clay

Sl. No.	Physical Properties of Soil	Soil Samples collected from actual site
1	Specific Gravity	2.65
2	Grain Size Distribution	Silt = 65.26% Clay = 33.38% Sand=1.36%

3	Silt Factor	0.229
4	Coefficient of Uniformity (Cu)	3.75
5	Coefficient of Curvature (Cc)	0.51
6	Permeability in cm/s	2.6×10^{-7}
7	Shear strength parameters	C = 1.2 kPa Ø = 14.1º
8	Liquid Limit	40.2
9	Plastic Limit	24.1
10	Plasticity Index	18.36
11	Standard Proctor OMC %	18.37
12	Standard Proctor MDD in kN/m^3	19.1

2.5 Preparation of model river bank and testing procedure

For both series-A and series-B, a meticulous approach was adopted to ensure the desired characteristics of the model banks. In series-A, cohesionless model banks were meticulously prepared with a uniform compaction energy of 0.209 kg/cm2. This process resulted in specific initial bulk densities tailored to moisture content (MC) levels of 13% and 6%. The banks were systematically constructed in three layers, with each layer subjected to 25 blows to achieve the targeted density. In series-B, the focus shifted to silty clay soil for the model banks. To attain the desired characteristics, an average density of 17.1 kN/m3 and 18.3 kN/m3 was meticulously achieved for moisture contents of 10% and 15%, respectively. The compaction energy of 0.209 kg/cm2 was applied to each layer during the preparation process, ensuring consistency and precision in the model's construction (Fig 3). These detailed preparation methods in both series aimed to create accurate representations of riverbanks, allowing for a comprehensive exploration of the influence of various factors on the failure mechanisms and profiles in the subsequent experimental investigations.

(a)

(b)

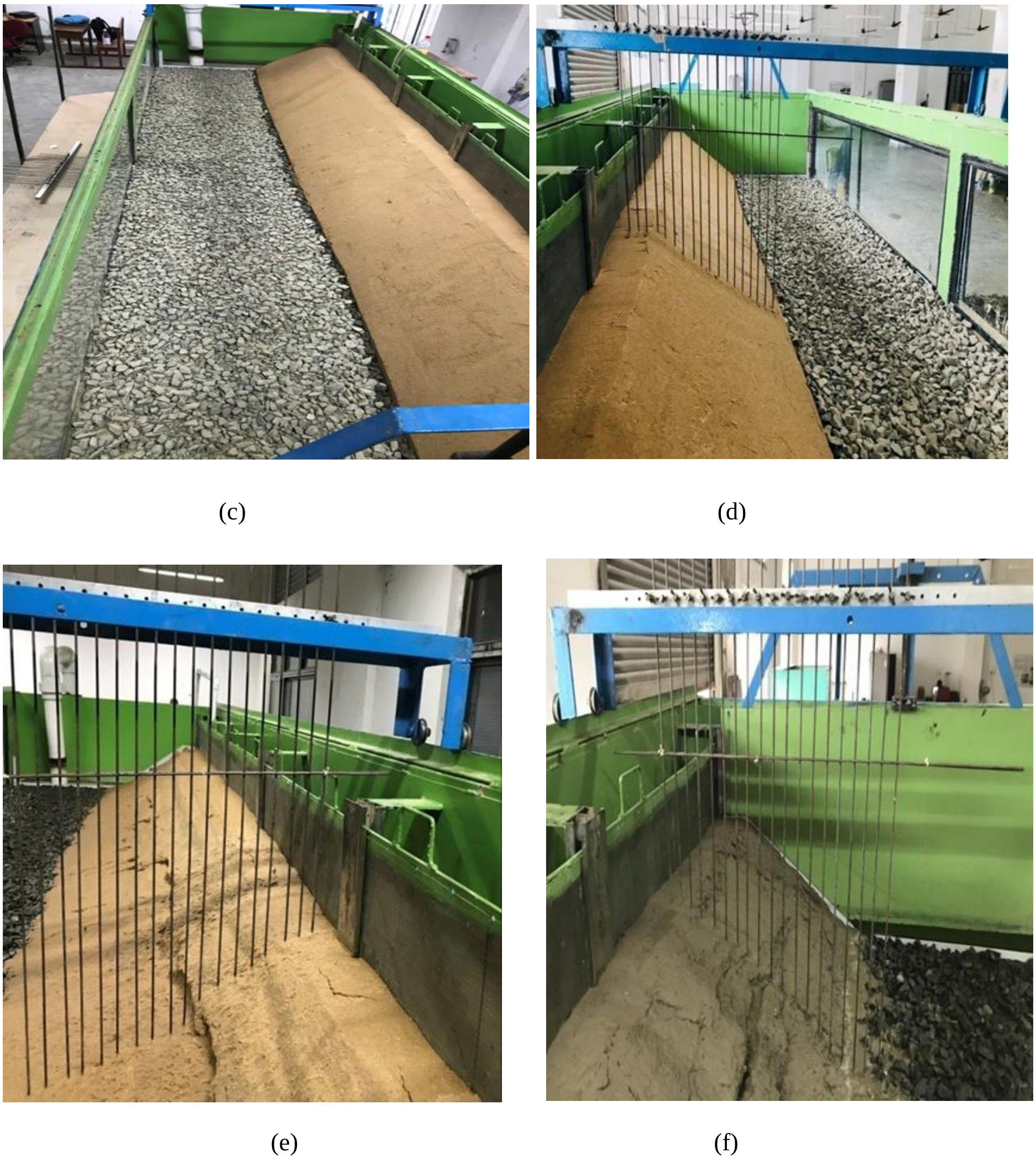

Fig. 3 model river bank (a) preparation of model bank (b) model bank prepared with silty clay (c) model bank prepared with sand (d) Initial profile of bank (e) Profile of bank after test(sand) (f) Profile of bank after test (Silty clay)

After the preparation of the model riverbank, an initial profile reading was taken by lowering the measuring gauge onto the surface of the model bank. These measuring gauges indicate the initial readings, which have been recorded. The pump started to fill the flume with water up to 50% and 80% of the model bank's height. To maintain the water at a specific height, the outer valve was opened. The surface velocity of the flowing water was measured using the floating method, registering a velocity of 6 cm/s inside the flume. After a 30-minute run of the flume, the pump was turned off, and drawdown occurred at a rate of 1 cm/s. Two flood heights (50% H & 80% H) were selected for drawdown in this study. The detailed experimental program has been tabulated below. (Table 5, Table 6)

Table 5 Summary of experimental runs for series-A.

Series-A							
Bank Material	**Slope**	**Moisture content %**	**Velocity of flow (cm/sec)**	**Flow time (min)**	**Drawdown ratios**	**Drawdown rate (cm/sec)**	**No. of Tests**
Cohesionless soil (sand)	1V:1.5H	6%	6cm/sec	30 min	50% H	1 cm/sec	3
					80% H		3
		13%			50% H		3
					80% H		3

Table 6 Summary of experimental runs for series-B.

Series-B							
Bank Material	**Slope**	**Moisture content %**	**Velocity of flow (cm/sec)**	**Flow time (min)**	**Drawdown ratios**	**Drawdown rate (cm/sec)**	**No. of Tests**
Silty clay	1V:1.5H	10%	6 cm/sec	30 min	50% H	1 cm/sec	3
					80% H		3
		15%			50% H		3
					80% H		3

3. Results and Discussions

A total 24 design experiment were conducted in the laboratory, encompassing variations in water levels, soil types, and moisture content. The data collected from these tests analysed to know the influence of different parameters namely. 1) Impact of bank material. 2) moisture content of model bank. 3) Variation in drawdown.

3.1 Presentation of results obtained from series-A (Cohesionless soil)

In this experimental series, twelve model tests were meticulously conducted using cohesionless soil, specifically sand, subjected to drawdown ratios of 50% H and 80% H concerning the model riverbank. The initial moisture contents were deliberately set at 6% and 13% to introduce variability in soil conditions. The ensuing alterations in the model riverbank's profile, post drawdown, are vividly depicted in the accompanying figure 4,5,6,7. During the 50% H drawdown with a 6% moisture content, the model riverbank exhibited minimal failure near its toe, and no significant failures were observed towards the crest. In stark contrast, the 80% H drawdown induced substantial failure in the middle of the bank slope, characterized by the sliding of the soil mass. Remarkably, the results underscore that the 80% H drawdown, coupled with a 6% moisture content, led to the most pronounced failure compared to the 50% H drawdowns, regardless of whether the moisture content was 6% or 13%. This observation suggests an increased vulnerability to failure under more significant drawdown conditions. Interestingly, the incremental increase in moisture content from 6% to 13% did not exert a significant impact on the extent of failures, irrespective of whether the drawdown was at 50% H or 80% H. This intriguing finding introduces a nuanced dimension to the relationship between moisture content and failure patterns under varying drawdown levels, emphasizing the intricate interactions within the modeled riverbank system.

These experimental results contribute valuable insights into the complex dynamics governing the stability and failure mechanisms of riverbanks exposed to diverse hydrological conditions. The study serves as a foundation for understanding how drawdown ratios and moisture content intricately influence the response of riverbanks, offering practical knowledge for the management and protection of riverbank environments. The nuanced understanding derived from this investigation lays a robust groundwork for further research aimed at enhancing our comprehension of the multifaceted interactions in geotechnical systems subjected to drawdown conditions.

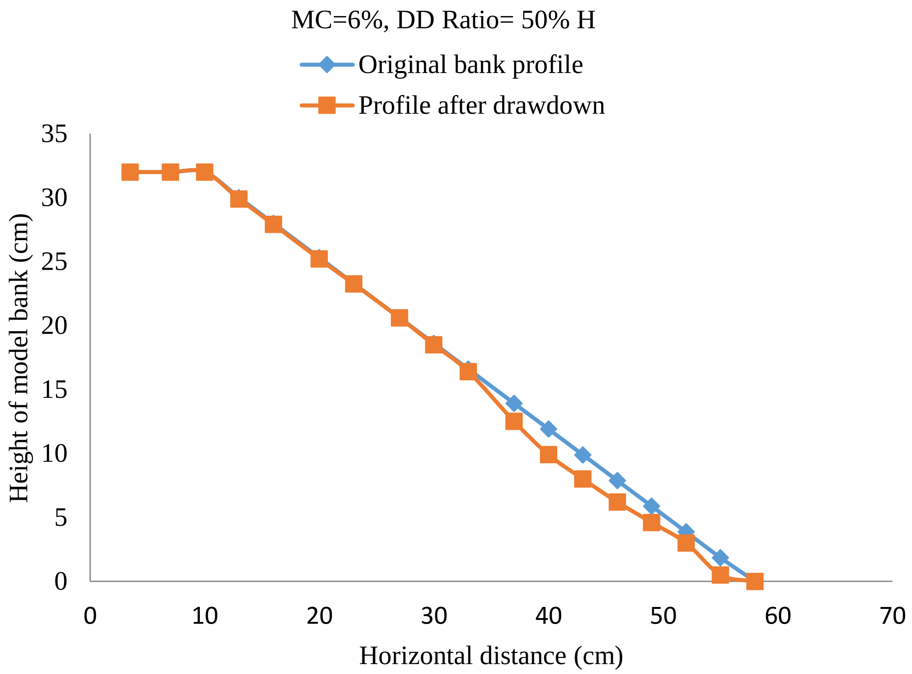

Fig. 4 Change of model riverbank profile after drawdown for 1V:1.5H slope, moisture content 6% and drawdown ratio 50% H.

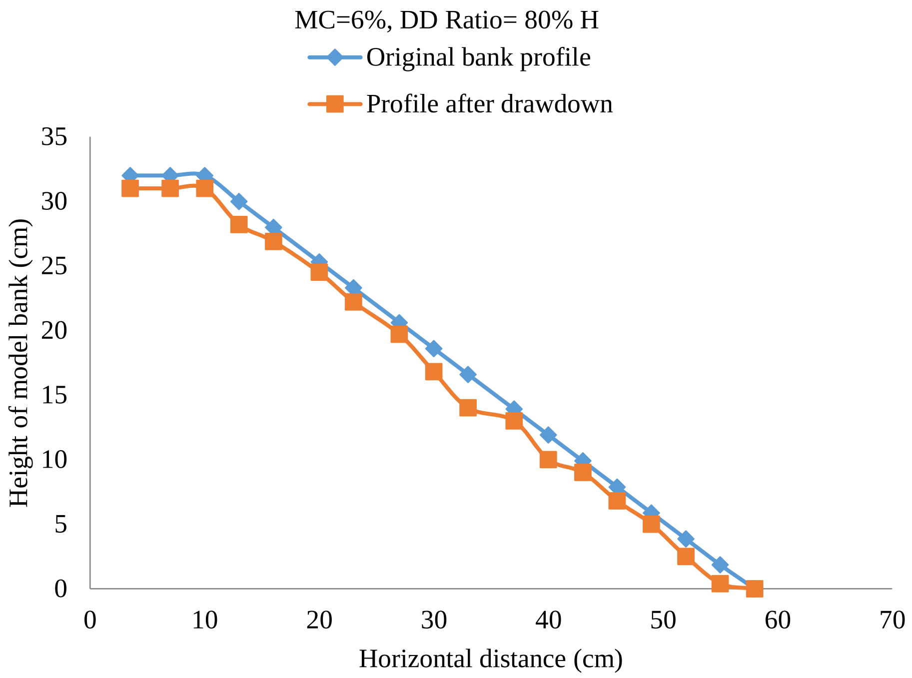

Fig.5 Change of model riverbank profile after drawdown for 1V:1.5H slope, moisture content 6% and drawdown ratio 80% H.

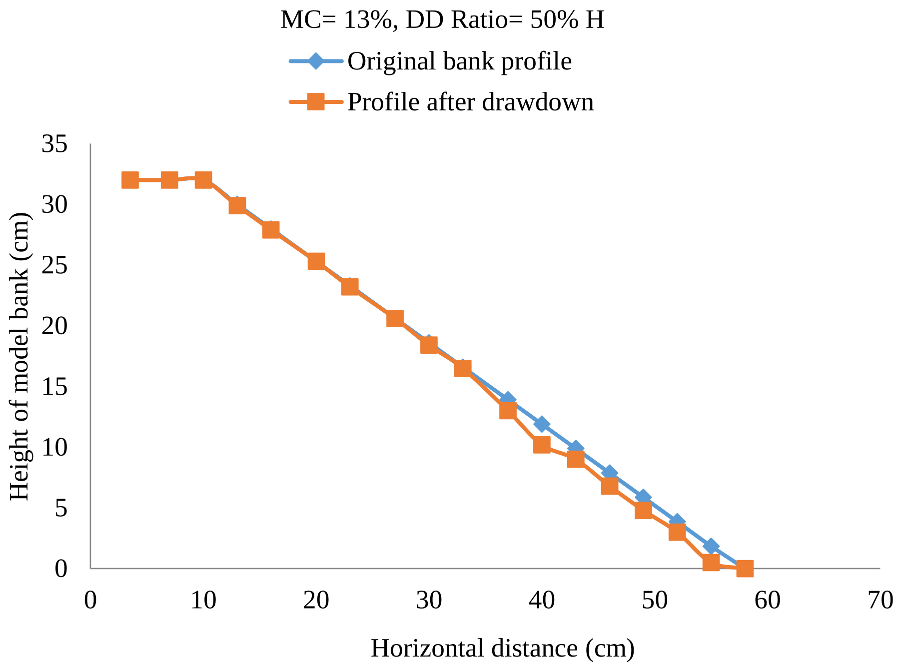

Fig. 6 Change of model riverbank profile after drawdown for 1V:1.5H slope, moisture content 13% and drawdown ratio 50% H.

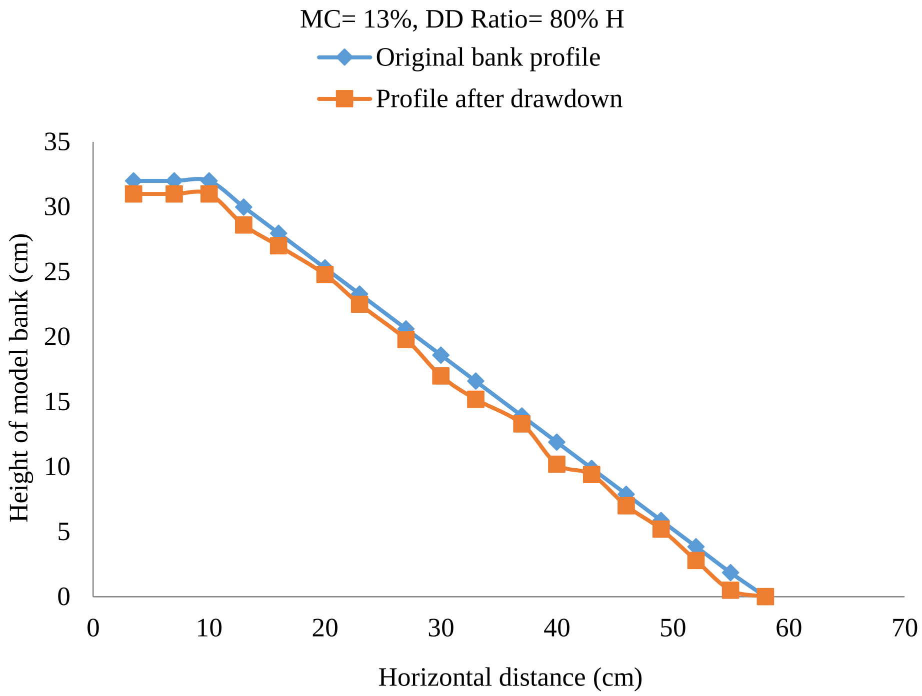

Fig. 7 Change of model riverbank profile after drawdown for 1V:1.5H slope, moisture content 13% and drawdown ratio 80% H.

A crucial aspect derived from this experimental study was the identification of the failure location and the initiation time of failure after drawdown (Table 7). Contrary to the anticipated synchronization between drawdown and bank failure, the results revealed a distinct pattern where the failure initiation did not strictly adhere to the drawdown timeline. Instead, failures commenced at various intervals after the initiation of drawdown, attributed to the expulsion of pore water from the bank.

Specifically, under a 50% H drawdown, failure locations were identified at distances of 21.57 cm and 10.74 cm from the bottom. The onset of failures occurred 25 seconds and 30 seconds after drawdown commencement for moisture contents of 6% and 13%, respectively. These finding challenges conventional expectations, suggesting that the immediate aftermath of drawdown does not precisely dictate the initiation of bank failure. The expulsion of pore water emerges as a pivotal factor influencing the temporal dynamics of bank stability. Expanding our scrutiny to an 80% H drawdown, failures manifested at locations 29.90 cm and 22.00 cm from the bottom. The initiation times were 25 seconds and 35 seconds after drawdown initiation for moisture contents of 6% and 13%, respectively. Remarkably, these results underscore that the 80% H drawdown, particularly with a 6% moisture content, represented the scenario with the most extensive failure pattern. This highlights the intricate interplay between drawdown levels, moisture content, and the subsequent stability of the modeled riverbank.

In essence, these findings deepen our understanding of the complex temporal and spatial dynamics governing riverbank stability under drawdown conditions. The delayed onset of failure, influenced by pore water expulsion, introduces a crucial nuance that necessitates a more comprehensive consideration of these interrelated factors in predictive models and risk assessments for riverbank management.

Table 7 Maximum failure zone after drawdown for cohesionless soil.

Moisture content %	Drawdown ratios	Drawdown rate (cm/sec)	Failure location from bottom (cm)	Starting time Failure time after d/d (sec)
6%	50% H	1 cm/sec	21.57	25
	80% H		29.90	20
13%	50% H		10.74	30
	80% H		22.00	35

3.2. Presentation of results obtained from series-B (Silty clay)

In this series featuring model banks constructed with silty clay, both 10% and 15% moisture contents exhibited minor erosion at 50% flow height. However, it is noteworthy that no substantial changes in slope were observed after the test. Therefore, the profile for this particular combination of the test is not presented, as the alterations in the bank's topography were not significant.

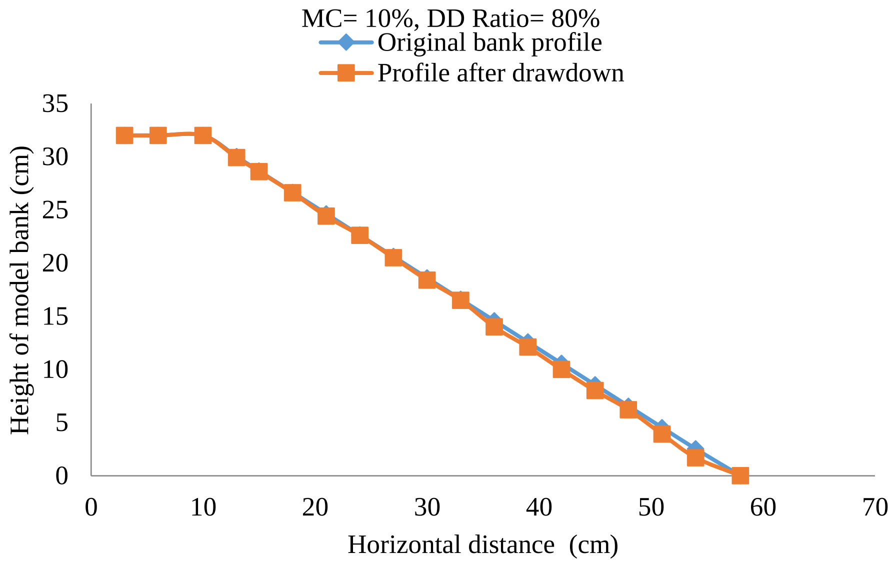

Fig. 8 Change of model riverbank profile after drawdown for 1V:1.5H slope, moisture content 10% and drawdown ratio 80% H.

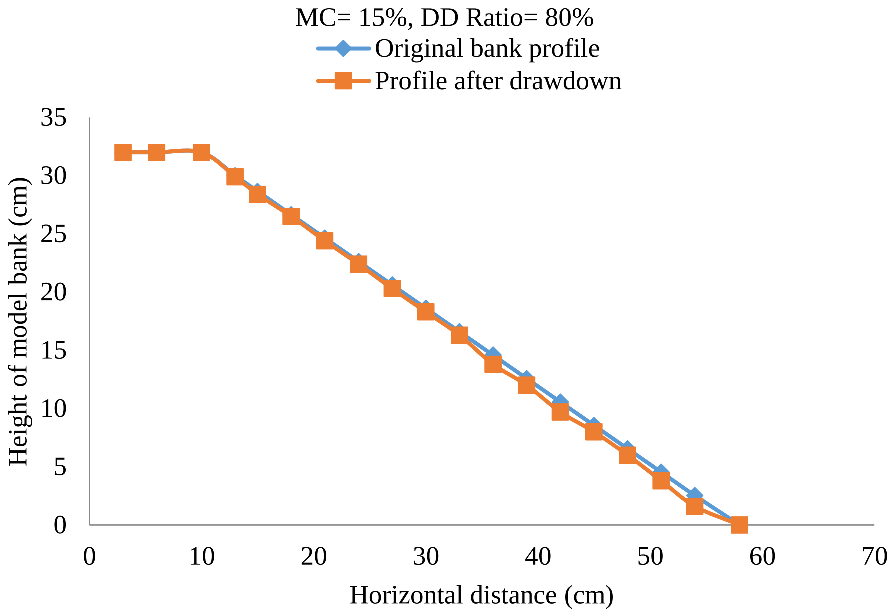

Fig.9 Change of model riverbank profile after drawdown for 1V:1.5H slope, moisture content 15% and drawdown ratio 80% H.

(a) (b)

Fig.10 (a) Failure crack (b) photo during the test.

Table 8 Failure location after drawdown for silty clay.

Moisture content %	Drawdown ratios	Drawdown rate (cm/sec)	Failure location from bottom (cm)	Starting time Failure time after d/d (sec)
10%	50% H	1 cm/sec	-	0
	80% H		15	45
15%	50% H		-	0
	80% H		20	60

At 80% flow height, there was partial erosion, and a longitudinal crack formed, as depicted in the figure 9,10. Additionally, it was observed that the failure location for an 80% drawdown initiated 15 cm and 20 cm from the bottom at times of 45 seconds and 60 seconds, respectively, as detailed in the table 8. The nature of silty clay soil is instrumental in shaping these observations. The forces propelling bank failure exhibit a diminished impact on erosion and failure in silty clay due to the internal cohesive action of the bank material effectively withstanding the seepage forces acting on the bank during water outflow after drawdown.Results shows that model bank made up of the sand shows the some what similar failure observed on the filed.

4. Conclusion

This study explores the outcomes of a series of physical model bank experiments designed to enhance our understanding of failure mechanisms in a laboratory setting that replicates real-world conditions. The experiments revealed several key findings: first, moisture content significantly affects the magnitude of failures, with cohesionless soil showing maximum failure at 6% moisture content under an 80% drawdown, while silty clay soil exhibited no significant failure. Second, a 50% drawdown had no notable impact on the model bank for either soil type. Third, the initiation of failure did not align strictly with the drawdown timeline; instead, failures occurred at varying intervals after drawdown initiation, attributed to the expulsion of pore water from the bank. Additionally, the model bank constructed with sand showed failure patterns somewhat similar to those observed in the field. Consequently, this study demonstrates that physical model studies can be effectively conducted prior to the execution of bank protection projects. The findings indicate that a model bank prepared with cohesionless soil provides a more accurate failure pattern than one prepared with cohesive soil under various geo-fluvial simulation constraints. Overall, these insights are crucial for informing bank protection strategies and improving the predictability of failure mechanisms in riverbanks, contributing to more effective and reliable engineering solutions in managing riverbank erosion and stability.

References

1) A. Recking, G. Piton, L. Montabonnet, S. Posi, A. Evette, *Design of fascines for riverbank protection in alpine rivers: Insight from flume experiments*, Ecological Engineering, **138**, 323-333, (2019)
2) K. Klavon, G. Fox, L. Guertault, E. Langendoen, H. Enlow, R. Miller, A. Khanal, *Evaluating a process-based model for use in streambank stabilization: insights on the Bank Stability and Toe Erosion Model (BSTEM)*. Earth Surf. Proc. Land. **42 (1)**, 191–213. https://doi.org/10.1002/esp.4073,(2017)
3) G. Gyssels, J. Poesen, E. Bochet, Y. Li, *Impact of plant roots on the resistance of soils to erosion by water: a review*. Prog. Phys. Geogr. **29 (2)**, 189–217. https://doi.org/10.1191/0309133305 pp443ra, (2005)
4) J.L. Florsheim, J.F. Mount, A. Chin, *Bank erosion as a desirable attribute of rivers.* Bioscience **58 (6)**, 519–529. (2008)
5) A. Recking, G. Piton, L. Montabonnet, S. Posi, A. Evette, *Design of fascines for riverbank protection in alpine rivers: Insight from flume experiments*. Ecological Engineering, **138**, 323-333., (2019)
6) T.K. Das, H.K. Halder, I.D. Gupta, *Forced Migration: Consequences of River Bank Erosion in India*. SSRN 1-19, (2013)

7) T.K. Das, H.K. Halder, I.D. Gupta, *Impact of riverbank erosion: A case study*. Australasian Journal of Disaster and Trauma Studies. **21(2).** (2017)
8) S. Mondal, P.P. Patel, I*mplementing Vetiver grass-based riverbank protection programmes in rural West Bengal, India*. Natural Hazards **103**:1051–1076. https://doi.org/10.1007/s11069-020-04025-5, (2020)
9) S. Khatun, A. Ghosh, D. Sen, *An experimental investigation on effect of drawdown rate and drawdown ratios on stability of cohesion-less river bank and evaluation of factor of safety by total strength reduction method*. International Journal of River Basin Management, **17(3)**, 289–299. (2019)
10) M.S. Islam, M.A. Matin, *Prediction of fluvial erosion rate in Jamuna River, Bangladesh*. International Journal of River Basin Management, **21(4)**, 625-637. (2023)
11) P. Sen, *River bank erosion and protection in Gangetic delta. River Bank Erosion and Land Loss*, a book published by Visva Bharati Publishing Department, Kolkata. (2008)
12) C. Parker, A. Simon, C.R. Thorne, The effects of variability in bank material properties on riverbank stability: Goodwin Creek, Mississippi. Geomorphology **101 (4)**, 533-543. (2008)
13) L. Nardi, M. Rinaldi, L. Solari, *An experimental investigation on mass failure occurring in a river bank composed of sandy gravel*. Geomorphology 163-164, 56-69. (2011)
14) M. Rinaldi, N. Casagli, *Stability of stream banks formed in partially saturated soils and effects of negative pore water pressures: the Sieve River (Italy).* Geomorphology **26**, 253–277. (1999)
15) M.A. Osman, C.R. Thorne, *Riverbank stability analysis I Theory*. ASCE Journal of Hydraulic engineering **114**: 134–150. (1988)